A mobility shift assay for DNA detection using nanochannel gradient electrophoresis

Michael A. Startsev,[†] Martin Ostrowski,[‡] Ewa M. Goldys,[†] and David W. Inglis[*¶]

Department of Physics and Astronomy, Macquarie University, Sydney, Department of Chemistry and Biomolecular Sciences, Macquarie University, Sydney, and Department of Engineering, Macquarie University, Sydney

E-mail: david.inglis@mq.edu.au

[*]To whom correspondence should be addressed

[†]Department of Physics and Astronomy, Macquarie University, Sydney

[‡]Department of Chemistry and Bimolecular Sciences, Macquarie University, Sydney

[¶]Department of Engineering, Macquarie University, Sydney 1

Keywords: Nanofluidics, electrophoresis, mobility, PNA

Total number of words: 3300

Abstract

Conventional detection of pathogenic or other biological contamination relies on amplification of DNA using sequence-specific primers. Recent work in nanofluidics has shown very high concentration enhancement of biomolecules with some degree of simultaneous separation. This work demonstrates the combination of these two approaches by selectively concentrating a mobility shifted hybridization product, potentially enabling rapid detection of rare DNA fragments such as highly specific 16s rDNA. We have performed conductivity gradient electrofocusing within nanofluidic channels and have shown concentration of hybridized peptide nucleic acids (PNA) and DNA oligomers. We also show selectivity to single base-pair mismatch on 18-mer oligos. This approach may enable sensitive optical detection of small amounts of DNA.

1 Introduction

Detection of DNA fragments is a significant problem in a wide range of areas including food safety, medicine and forensics. The most common techniques for detecting DNA fragments involve amplification of specific sequences using polymerase chain reaction (PCR) primers. However there is ongoing interest in alternative, rapid techniques that avoid amplification and are compatible with the lab-on-a-chip, especially for point of care systems where time is critical. Samples that contain a low concentration of the DNA fragments are of special interest and present an even greater challenge in such lab-on-chip systems because of slow reaction kinetics and low signal levels.

Rapid detection of analytes with low concentration is usually addressed by reporter signal amplification. This includes catalysis (horseradish peroxidase, [1 Liu and Zhang, 2015]) and fluorescence enhancement [2 Zhao 2015]. These techniques are vital, but sensitivity is always limited by sample concentration. Pre-concentration prior to separation can help but may lead to precipitation of high abundance compounds, disrupting the separation process.

To overcome this, simultaneous concentration and separation of target molecules is required. A number of groups have pursued this approach which can potentially yield vastly improved sensitivity. Simultaneous concentration and separation has been achieved with micro-organisms using dielectrophoresis [3], with chiral compounds using temperature gradient focusing [4], and with small molecules using a bipolar electrode [5]. DNA in complex mixtures has been separated and concentrated using isotachophoresis [6]. Recently, nanofluidic approaches to simultaneous concentration and separation have been demonstrated, including separation of amino acids by depletion zone isotachophoresis [7], and previous work by our group to separate proteins [8,9].

In this work we show that gradient electrophoresis in a nanofluidic channel described in reference [8] can be used to focus DNA and, simultaneously, detect a single base pair

mismatch between a PNA-DNA hybrid. This was demonstrated with a 16S ribosomal RNA gene sequence from *Bacillus cereus*, a model organism. This binding to a PNA label makes it possible to identify a specific DNA sequence initially present in the sample at low levels.

2 Theory

Figure 1 shows how changes to molecular mobility upon molecular binding can be exploited in order to make DNA:PNA hybridization detectable within the nanochannel conductivity gradient scheme.

Unlike DNA, PNA does not carry a charge on its backbone so it has an electrophoretic mobility μ_{PNA} that is expected to be lower than the mobility of DNA. Successful hybridization of PNA to DNA results in a modified charge to mass ratio of the DNA:PNA complex. PNA binds to nucleic acids in a complimentary sequence-specific fashion. Using PNA as a molecular probe instead of oligonucleotides allows for robust and highly specific binding [10-14] while producing a complex with a mobility shift that can potentially be separated by electrophoretic techniques.

The separation and concentration principle is shown in Figure 1. The electroosmotic force varies along the channel length due to changing field strength and double layer thickness. The electroosmotic velocity at the channel surface also varies; however, conservation of mass requires that net fluid transport for a rectangular channel must be the same along the channel length. The validity of this simplistic model can be assessed by considering the Péclet number (Equation 1).

$$P_e = {Lu}/{D} \tag{1}$$

The Péclet number is the ratio of advective transport to diffusive transport. In our case the length scale, L, is the channel thickness (100 nm), D is the diffusion coefficient for the oligomer (approximately 6 $\mu m^2/s$), and u is the net velocity, which is of the order 50 $\mu m/s$. This gives the value of P_e = 0.8. This means that the macromolecule's diffusive transport is slightly more significant than the advective transport, and therefore the substantial complexities of the electroosmotic and electrophoretic forces, which vary with depth are averaged by diffusion. This allows us to assume that the electroosmotic (EO) force is constant along a rectangular nanochannel. The blue line in the figure indicates this constant, depth-averaged EO force. The force from electrophoresis (EP) is variable, being stronger at the low conductivity (high electric field) end of the nanochannel. For negatively charged particles EP has the opposite direction to EO. A stable equilibrium position exists for all negatively charged molecules where net force is equal to zero (indicated by the intersection of the EO and EP lines for that particular molecular mobility). Molecules with higher mobility are trapped closer to the low salt, cathodic end, while low mobility molecules are trapped closer to the high salt, anodic end. The differences in mobility result in molecules with different charge to molecular weight ratio being trapped in different locations along the channel (dotted cyan). It is reasonable to expect

three different focusing positions within the channel: one for PNA, one for DNA and one for PNA:DNA hybrid molecules. The width of the focus band is increased by diffusion and reduced by a steep conductivity gradient. While the above analysis is qualitative, more complete theoretical treatments of the opposing electroosmotic and electrophoretic effects in the nanochannel are given in References [15-17].

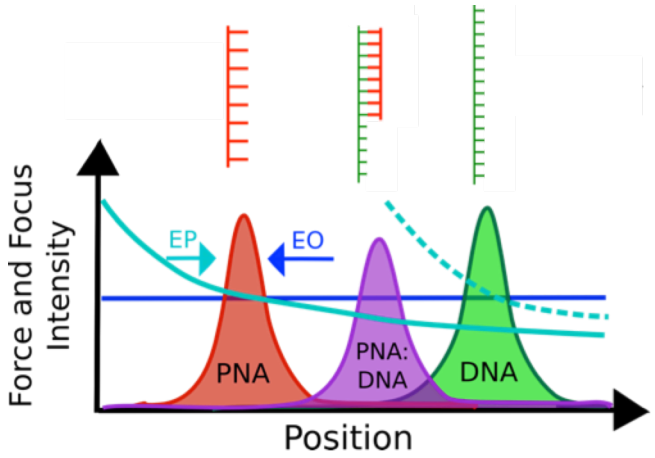

Figure 1: Illustration of proposed scheme for hybridization detection. PNA and DNA have distinctly different mobilities μ. An EP force acts on individual biomolecules and is increased in areas of low conductivity. The EO force opposes the EP. If PNA and DNA are hybridized, the mass and charge of the molecule will be modified and there will be a new trap location for the complex.

3 Materials and methods

3.1 Device fabrication

The device is very similar to that used in reference [8], a p-type, 1-10 Ohm.cm, <100> silicon wafer with a 50 nm oxide was used as a substrate. The microchannels were photolithographically patterned and the oxide was etched using CF_4 plasma. The wafer was coated with SU-8 and office tape to protect it during sand-blasting of through-holes. After cleaning, the microchannels were wet-etched using potassium hydroxide and 2-propanol to a depth of 6 to 10 μm. The remaining oxide was then stripped using hydrofluoric acid and approximately 120 nm of new thermal oxide was grown. Nanochannels of 200 μm length which connect the microchannels were then photolithographically patterned and etched in CF_4 plasma to a depth of 86 ± 4 nm. The nanochannels tapered from 15 μm wide at the high salt (+ve) and to 10 μm wide at the low salt (-ve) microchannel. Finally, a 300 μm thick, 76.3 mm wafer of thermal expansion matched borosilicate glass was bonded to the silicon wafer using a reverse RCA procedure.

3.2 Conductivity gradient electrofocusing

The conductivity gradient was formed by introducing a constant flow of two different phosphate buffers through the two microchannels. This fixed either end of the nanochannels to dissimilar salt concentrations. The positive microchannel received phosphate buffer with NaCl added to raise the concentration to 241 mM NaCl. The negative microchannel received phosphate buffered saline that had been diluted to 24 mM NaCl. A conductivity gradient therefore exists in the nanochannel, and remains there under small voltages and where ion or mass transport by electroosmosis in the nanochannels does not overwhelm mass transport in the microchannels [18].

Buffer flow at the microchannel ports was driven by surface tension. Approximately 10 µl droplets of buffer or analyte sample were pipetted onto the inlets of each microchannel. Every 10-20 minutes, the droplets were refreshed to minimize changes in salt concentration due to evaporation. Between each trial the channels were flushed with de-ionized water and phosphate buffer solutions that matched the conductivity to be used in the next trial. Silver-silver chloride wire electrodes were placed in the inlet and outlet ports of both high salt and low salt microchannels.

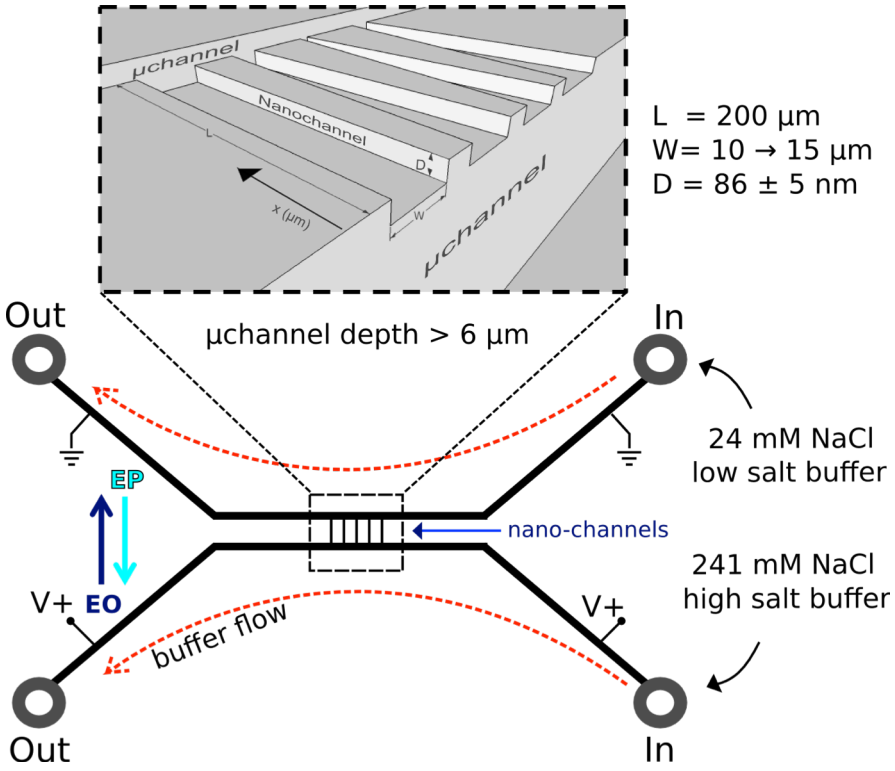

Figure 2: Schematic of the nanochannel device. The inset describes the dimensions of the nanochannels. The length of the nanochannels are 200 μm, The nanochannel width is tapered from 10 to 15 um, and the depth is 86 nm. The low salt and high salt buffer droplets are introduced to the ground and V+ (+ve bias) microchannel inlets respectively. Within the nanochannels, electrophoresis force (EP) is directed toward the +ve electrode and electroosmosis force (EO) is directed toward the -ve electrode.

3.3 Analyte preparation

A single-stranded 18-mer PNA probe (probe 1) (Invitrogen - Life Technologies) was selected to compliment the 16S ribosomal RNA gene sequence from *B. cereus* (ATCC14579 strain). The sequence (00393 [19]) was chosen from several candidates on ProbeBase according to the criteria for successful PNA production. These rules eliminated all but one sequence due to the possibility of self hybridization of the probe. A single base mismatch strand of PNA probe was also generated (probe 2) along with a single stranded oligonucleotide identical to the 16S rRNA sequence (Oligo). The sequences of PNA-probe-1, PNA-probe-2 and rRNA-mimic oligo are displayed in Table 1.

Name	Terminus	Sequence	Terminus
Probe 1	Alexa 555	5’ - TG CGG TT**C** AAA ATG TTA T - 3’	-
Probe 2	Alexa 555	5’ - TG CGG TT**G** AAA ATG TTA T - 3’	-
Oligo	-	3’ - AC GCC AA**G** TTT TAC AAT A - 5’	fluorescein 488

Table 1: Oligonucleotide:PNA Hybridization sequences.

The oligonucleotides and probes were imaged under an inverted fluorescence microscope with a cooled monochromatic camera and filter cubes with single band excitation filters. In this way, the signals from fluorescein-labeled oligonucleotides and Alexa Fluor-labeled PNA could be observed independently of one another. Hybridization of PNA and oligonucleotides was straightforward due to both species having single stranded base pair chains. The process consisted of mixing PNA and oligonucleotides at 1:1 molar ratio, followed by heating and mixing for 10 minutes. After cooling at 4˚C for 30 minutes, the hybridized analyte was taken to be used in either gel electrophoresis trials or nanochannel electrofocusing trials.

3.4 Genomic DNA shearing

The mobility shift method requires that an 18mer PNA oligo changes the mobility of a DNA fragment. To do this, the fragment must be small. Shearing of DNA also enables more reliable transport through the nanochannels. *B. cereus* DNA was sheared on a Covaris E220 Ultrasonicator at the University of New South Wales (UNSW). The length of the resultant DNA was estimated with an Agilent Bioanalyzer 2100 and confirmed to be a distribution spanning between 50 - 250 bp, peaking at 150 bp.

3.5 Polyacrylamide gel electrophoresis

While agarose gels can successfully separate DNA fragments of 50-20,000 bp, polyacrylamide gels have a considerably higher resolving power for small 5-500 bp fragments of DNA and are more suitable for analyzing short DNA fragments. Polyachrylamide pre-cast mini-PROTEAN 10% TBE electrophoresis gels were purchased from Biorad inc. Analytes were mixed into a standard electrophoresis loading buffer, composed of 60% glycerol, 10 mM Tris, 60 mM EDTA and a colorant, bromophenol blue at 0.2% set to a pH of 8.3. Then the electrophoresis gel cast was inserted into a Mini-PROTEAN Tetra electrophoresis cell and a voltage of 100 V was applied for 50 minutes. An image of the focusing was then taken under an open Ultra-Lum transilluminator with a standard cell phone camera (Android Nexus 5).

4 Results and discussion

4.1 Separation of sheared genomic DNA from PNA

Before attempting to hybridize single stranded DNA (ssDNA) oligos to PNA, simultaneous concentration and separation of sheared double stranded *B. cereus* DNA (dsDNA) and PNA probe 2 was performed within the nanochannels at 0.4 V. Both DNA and PNA were supplied through the high conductivity (241 mM NaCl) end of the channel. During focusing, fluorescence images of Alexa Fluor 555 (bound to PNA probes) and SYBR Green I (which specifically binds to dsDNA) were taken in alternating 30 s intervals at 1 s exposure.

The dsDNA was not heated to the point of denaturing, so PNA had no access to binding sites and hybridization is not expected. Figure 3 shows the behaviour of the PNA and dsDNA bands. dsDNA shows a much higher concentration enhancement than PNA (2000 vs 500 for DNA and PNA respectively). This difference could be attributed to a higher initial concentration of SYBR green compared with Alexa Fluor bound to the PNA probe. Note that when run at the same time as the sheared DNA, the PNA is trapped much closer to the (high salt, left) side, than when PNA is run by alone or with complimentary ssDNA oligos. The reason for this is not clear.

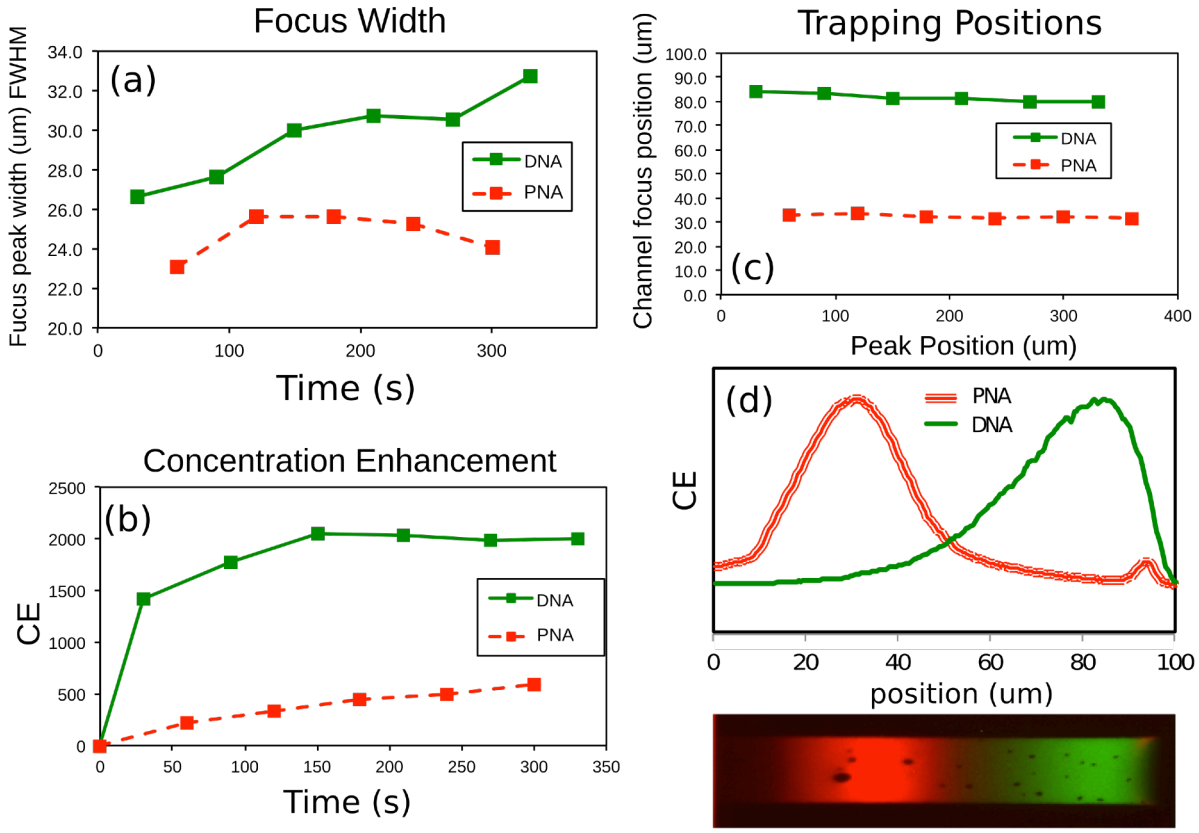

Figure 3: a) The full-width-half-max measure of the bands forming within the nanochannel over time. (b) The concentration enhancement factors for DNA and PNA-probe 2 over time. (c) the stable focus positions for DNA and PNA probe-2 over time. (d) The focus profiles (normalized) for PNA probe-2 and DNA in the nanochannel.

4.1 Detection of DNA:PNA complex

Figure 4 shows our central result, the detection of a single base pair mismatch in a DNA:PNA complex. We repeatedly use the nanochanel device to focus oligo:PNA-Probe-1 hybrids and oligo:PNA-Probe-2 hybrids at 12-μM:12-μM concentration ratios (both single stranded). Three non-successive repetitions of the focusing data were collected and the degree of "overlap" was calculated in order to quantify the difference made by a G-G base-pair mismatch (full sequences shown in Table 1). Overlap is defined as the percentage of the area under the curve that is shared by both red and green intensity plots. Clearly separated peaks would

show a very low level of overlap, whereas a single molecular species with two fluorescent tags would show 100% overlap. The blue column in Figure 3 titled “Probe-2 Oligo (mix)” was used as a control in which the oligonucleotide PNA had minimal time to hybridize before focusing, having experienced no heating or shaking, as it was combined immediately before pipetting on to the chip.

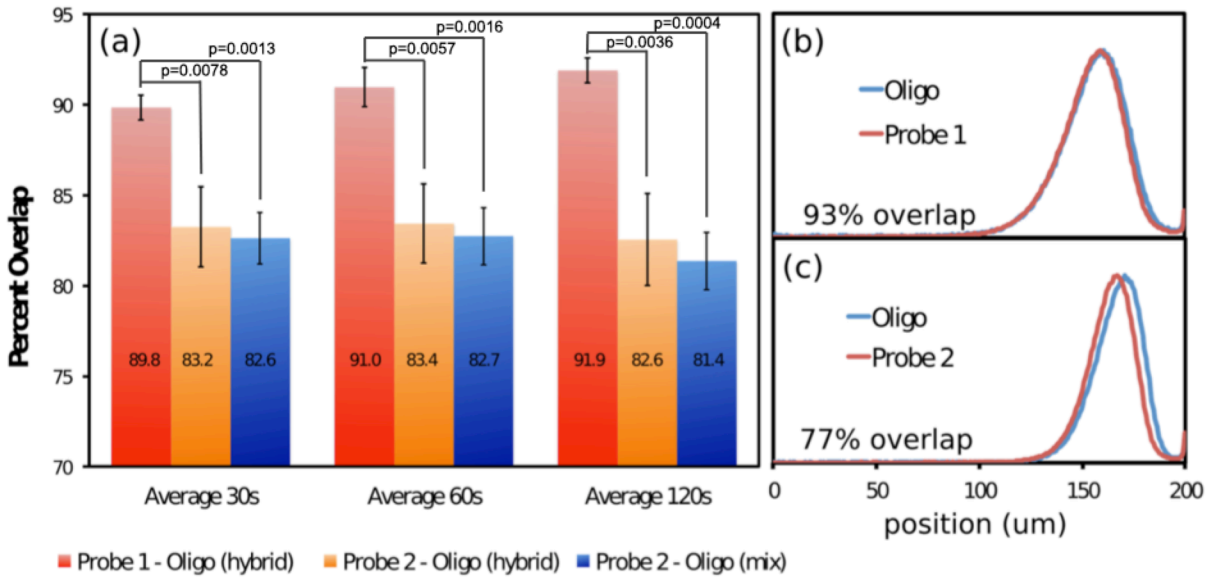

Figure 4: a) Comparison of overlap of focus bands for hybridization of matched (Probe 1-Oligo) and unmatched (Probe 2-Oligo) hybridization versus time in the nanochannel device. PNA-Probe-1 shows a consistently higher percent overlap compared to PNA-Probe-2. (b) Example of PNA probe 1 overlap (normalized). (c) Example of PNA probe 2 overlap (normalized).

The oligo:PNA-probe-1 overlap was consistently around 90% at all time points (30,60 and 120 s) (Figure 4). The oligo:PNA-probe-2 hybrid with the G-G base pair mismatch was found to be around 83%, and the control group (mismatch sequence with no hybridization) produced peaks which had approximately 82% overlap.

The degree of separation between the mismatched fragments (orange and blue bars) is small, but it is statistically greater than for the matched fragments (red bars), which show approximately 90% overlap. This suggests the system is able to differentiate the single base mismatch over an 18-mer oligo and 18-mer probe. This high level of specificity is desirable to reduce the rate of false positives in detecting any dangerous pathogen. The roughly 80% overlap for the mismatched set (orange and blue bars) is likely caused by the similar focus position observed for the two molecules. Some overlap is also likely caused by the binding affinity of the mismatch pair, which is significant. This could certainly be improved with an experimental design using a probe with a substantially different electrophoretic behavior than the target sequence. This could possibly be achieved using a positively charged fluorescent label.

4.2 PNA mobility characterization

Figure 5 shows focusing data of various input concentrations of PNA when introduced into the high salt (+ve) microchannel. Figure 5(a) shows that PNA at 1.0 μM concentration yields the highest concentration enhancement factor (CE). Here, CE is defined as the intensity of fluorescence in the band divided by the intensity in the microchannel times the micro channel to nanochannel depth ratio. Figure 5(b) shows the peak positions of each of the concentrations of PNA, measured from the high salt end of the 100 μm long nanochannel. Figure 4(c) shows the full-width-half-max of the bands versus time. We expected PNA to carry a slightly positive charge but observed that it focused in the nanochannels under an applied positive voltage in much the same way as negatively charged DNA oligonucleotides of the same length.

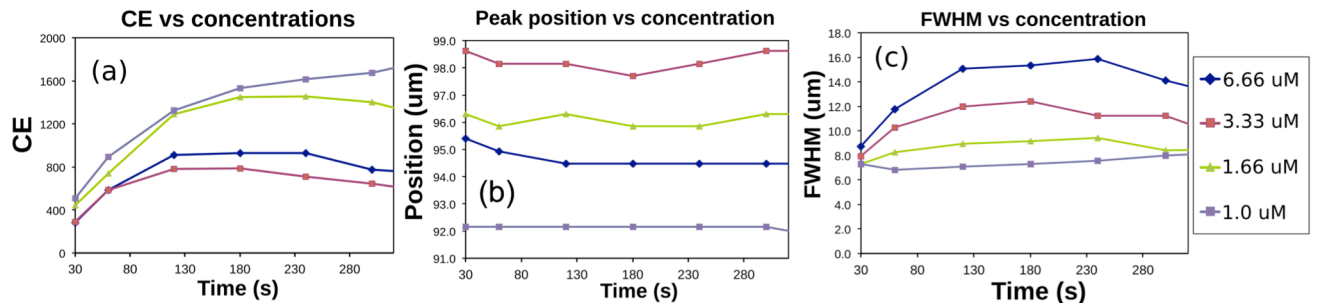

Figure 5: Contrary to our initial expectations, the PNA probes focused in our nanochannel. (a) Concentration enhancement (CE) over time for different PNA initial concentrations. (b) Focus peak positions over time. (c) The width of peaks (FWHM) for each initial PNA concentration. The concentrations 6.66, 3.33, 1.66, 1.0 μM correspond to 37.4, 18.7, 9.0, 5.6 μg/mL respectively.

4.4 Gel and nanochannel gradient electrophoresis

Figure 6 shows results of nanochanel electrofocussing and gel electrophoresis of the pure and hybridized samples over a range of concentrations. The right side shows a region of the gel containing PNA probe 1, the oligonucleotide, and PNA hybridized to the oligonucleotide. The gel electrophoresis bands are observed to run almost twice as far as the 200 bp band in a dsDNA ladder. This is as expected for the oligonucleotides, but entirely surprising for the PNA. The hybridized molecule unsurprisingly runs to about the same position, and shows a high degree of overlap.

The left side of Figure 6 shows the same samples in the nanochannel device. In both the nanochannel device and the gel, DNA and PNA behave very similarly. However we see in the nanochannel that the DNA and PNA form peaks that are more resolved than in the gel. The short DNA oligos form a narrower band in the nanochannel than the sheared genomic DNA (Figure 3).

We observe that the PNA and DNA oligos behave in much the same way in both the nanochannel device and the gel. One possible explanation is that the labeled PNA molecules are acquiring negative charge within the buffers. While this effect needs further investigation to be fully explained, it does not invalidate our key result, the differentiation of the match and miss-match strands.

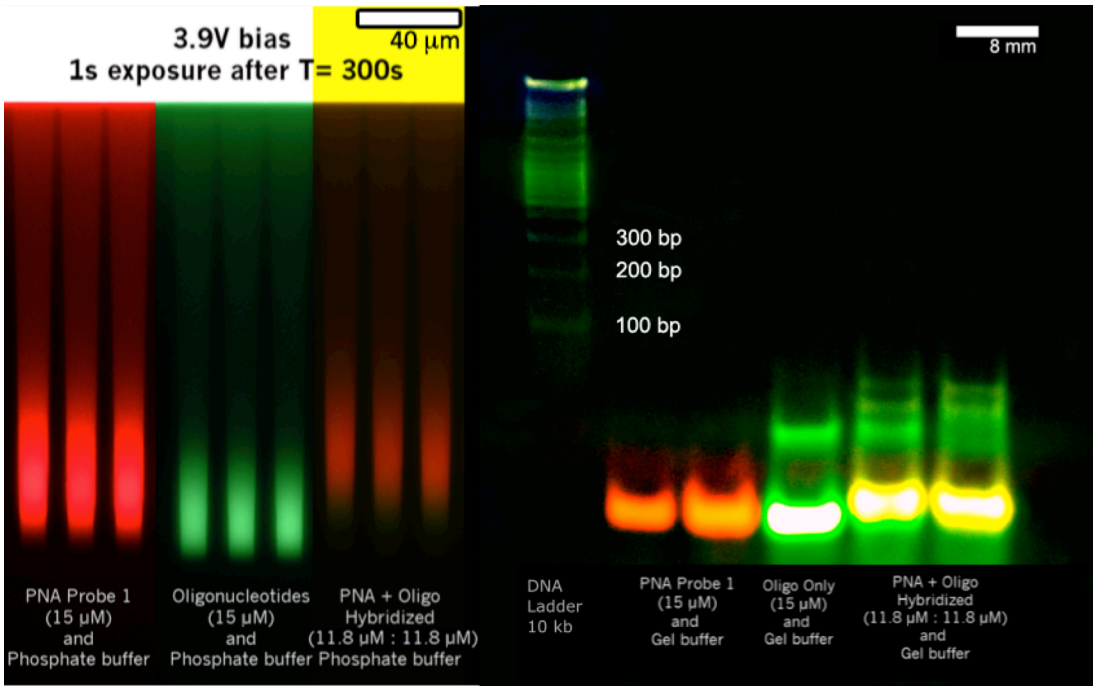

Figure 6: RIGHT: Polyacrylamide gel electrophoresis of ladder, probe 1, oligo, and hybridized sample. The rightmost yellow bands indicate hybridization between the red (Alexa Fluor 555 labeled PNA) and green (fluorescein 488 labelled oligonucleotides). LEFT: The same focusing experiment replicated within the nanochannel device. In the nanochannel device, focussed bands are formed in much less time than it takes to run the gel, and the probe and oligo are better separated than in the gel.

5 Concluding remarks

This work is motivated by the need to detect small amounts of free DNA and the potential of detecting a mobility shift using simultaneous concentration and separation in a nanochannel. We have demonstrated a novel nanofluidic focusing scheme to detect hybridization of peptide nucleic acid (PNA) with DNA. A green 18-mer DNA oligo hybridized to a complementary red 18-mer PNA probe and produced a band with a high degree of red-green overlap (92%). This overlap reduced to 83% when using a PNA probe with a single base pair mismatch demonstrating that the system is capable of discriminating a single base pair mismatch. Contrary to expectations, we found that PNA oligos behaved as negatively charged species, focusing as well in the nanochannel as DNA and demonstrating the same electrophoretic mobility in a polyacrylamide gel electrophoresis as the DNA oligos.

Acknowledgement

This work was supported by the Australian Research Council (DP110102207). Device fabrication was carried out with assistance from the University of New South Wales node and the South Australian node of the Australian National Fabrication Facility, established under the NCRIS scheme. The authors declare no conflicts of interest.

References:

[1] Liu, F., Zhang, C., Sensors and Actuators B: Chemical, 2015, 209, 399-406.
[2] Zhao, H., Wang, L., Zhu, J., Wei, H., Jiang, W., Talanta, 2015, 138, 163-168.
[3] Moncada-Hernández H., Lapizco-Encinas B.H., *Anal. Bioanal. Chem*. 2010 396(5), 1805-16.
[4] Balss, K.M., Vreeland, W.M., Phinney, K.W., Ross D., *Anal. Chem.*, 2004, 76 (24), 7243–7249.
[5] Laws, D.R., Hlushkou, D., Perdue, R.K., Tallarek, U., Crooks, R.M., *Anal. Chem.*, 2009, 81(21), 8923–8929.
[6] Bercovici, M., Kaigala, G.V., Mach, K.E., Han, C.M., Liao, J.C., Santiago J.G., *Anal Chem.* 2011, 83(11), 4110–4117.
[7] Quist, J., Janssen, K.G.H, Vulto, P., Hankemeier, T., van der Linden, H.J., *Anal. Chem*., 2011, 83, 7910–7915.
[8] Inglis, D.W., Goldys, E.M., Calander, N.P., *Angew. Chem. Int. Ed.,* 2011, 50, 1–6.
[9] Startsev, M.A., Inglis, D.W., Baker M.S., Goldys E.M., *Analytical Chemistry*, 2013, 85/15, 7133-7138.
[10] Nielsen P.E., Egholm, M., Berg R.H., Buchardt, 0., *Science*, 1991, 254(5037), 1497–1500.
[11] Nielsen, P.E., Egholm, M. et al., *Current Issues in Molecular Biology,* 1999, 1(2),89–104.
[12] Zhang, N. Apella, D.H., *Journal of Infectious Diseases*, 2010, 201(Supplement 1), S42–S45.
[13] Nielsen, P.E., *Peptide Nucleic Acids: Protocols and Applications*. Horizon Bioscience. Great Britain 2004.
[14] Egholm, M., Buchardt, O., Christensen, L., Behrens, C., Freier, S.M., Driver, D.A., Berg, R.H., Kim, S.K., Norden, B. and Nielsen, P.E., Nature, 1993, 365, 556-568.
[15] Hsu, WL., Harvie, D.J.E., Davidson, M.R., Jeong, H., Goldys E.M., Inglis D.W., *Lab Chip*, 2014, 14(18), 3539-49.
[16] Hsu, WL., Inglis D.W., Startsev, M.A., Goldys E.M., Davidson, M.R., Harvie, D.J.E., *Analytical Chemistry*, 2014, 86, 8711-8718.
[17] Yuan, Z., Garcia, A. L., Lopez, G. P., Petsev, D. N., *Electrophoresis*, 2007, 28, 595–610.
[18] Hsu, WL., Inglis, D.W., Jeong, H., Dunstan, D., Davidson, M.R., Goldys, E.M., Harvie, D.J.E., *Langmuir*, 2014, 30(18), 5337-5348.
[19] Liu W.-T., Mirzabekov A. D., Stahl D. A., *Environ. Microbiol.*, 2001, 3, 619-629.